Title

Metamorphosis of the Drosophila visceral musculature and its role in intestinal morphogenesis and stem cell formation

Journal

Developmental Biology, 420(1)

ISSN

0012-1606

Authors

Aghajanian, Patrick
Takashima, Shigeo
Paul, Manash
et al.

Publication Date

2016-12-01

DOI

10.1016/j.ydbio.2016.10.011

Peer reviewed

HHS Public Access

Author manuscript

Dev Biol. Author manuscript; available in PMC 2017 December 01.

Published in final edited form as:

Dev Biol. 2016 December 01; 420(1): 43–59. doi:10.1016/j.ydbio.2016.10.011.

Metamorphosis of the *Drosophila* visceral musculature and its role in intestinal morphogenesis and stem cell formation

Patrick Aghajanian, **Shigeo Takashima**, **Manash Paul**, **Amelia Younossi-Hartenstein**, and **Volker Hartenstein***

Department of Molecular Cell and Developmental Biology University of California Los Angeles, Los Angeles, CA 90095

Abstract

The visceral musculature of the *Drosophila* intestine plays important roles in digestion as well as development. Detailed studies investigating the embryonic development of the visceral muscle exist; comparatively little is known about postembryonic development and metamorphosis of this tissue. In this study we have combined the use of specific markers with electron microscopy to follow the formation of the adult visceral musculature and its involvement in gut development during metamorphosis. Unlike the adult somatic musculature, which is derived from a pool of undifferentiated myoblasts, the visceral musculature of the adult is a direct descendant of the larval fibers, as shown by activating a lineage tracing construct in the larval muscle and obtaining labeled visceral fibers in the adult. However, visceral muscles undergo a phase of remodeling that coincides with the metamorphosis of the intestinal epithelium. During the first day following puparium formation, both circular and longitudinal syncytial fibers dedifferentiate, losing their myofibrils and extracellular matrix, and dissociating into mononuclear cells ("secondary myoblasts"). Towards the end of the second day, this process is reversed, and between 48 and 72h after puparium formation, a structurally fully differentiated adult muscle layer has formed. We could not obtain evidence that cells apart from the dedifferentiated larval visceral muscle contributed to the adult muscle, nor does it appear that the number of adult fibers (or nuclei per fiber) is increased over that of the larva by proliferation. In contrast to the musculature, the intestinal epithelium is completely renewed during metamorphosis. The adult midgut epithelium rapidly expands over the larval layer during the first few hours after puparium formation; in case of the hindgut, replacement takes longer, and proceeds by the gradual caudad extension of a proliferating growth zone, the hindgut proliferation zone (HPZ). The subsequent elongation of the hindgut and midgut, as well as the establishment of a population of intestinal stem cells active in the adult midgut and hindgut, requires the presence of the visceral muscle layer, based on the finding that ablation of this layer causes a severe disruption of both processes.

*Corresponding author: volkerh@mcdb.ucla.edu.

Keywords

visceral muscle; lineage; intestine; metamorphosis; *Drosophila*

Introduction

The insect intestine is formed by a monolayered epithelium of enterocytes, surrounded by a layer of striated visceral muscle cells. Foregut and hindgut possess only circular muscles, whereas the midgut features a layer of circular muscles, flanked by longitudinal fibers; circular and longitudinal visceral muscles form an interwoven contractile network responsible for gut motility (Hartenstein, 2005; Schröter et al., 2006; Fig. 1A–C). In *Drosophila*, circular fibers of both larval and adult gut are composed of two cells each, one cell located on the right side, the other on the left side of the gut (Fig. 1D, D′). Individual circular visceral muscle cells themselves are small syncytia, each containing two nuclei (Fig. 1D). Longitudinal fibers of the midgut are also formed by syncytial cells, each containing 3–5 nuclei; several of these syncytia attach end-to-end to form an elongated fiber that extends uninterruptedly along the entire length of the midgut tube. Individual muscle fibers contain ~4–6 striated myofibrils (Fig. 1E). Each myofibril is formed by a dense and regularly patterned array of myofilaments (Fig. 1F). Muscle fibers are surrounded on all sides by a basement membrane (Fig. 1F).

The early development of the visceral muscle of the insect model system *Drosophila* has been analyzed in considerable detail (Bate, 1993; Azpiazu and Frasch, 1993; Maggert et al., 1995; Lee et al., 2003; reviewed in Hartenstein and Chipman, 2016). Visceral muscle is derived from the lateral part of the mesoderm, the so-called visceral mesoderm, which attaches to the developing gut tube during mid stages of embryogenesis, very similar to the formation of the splanchnopleura that gives rise to the visceral muscle in vertebrates (Tribioli et al., 1997). The *Drosophila* visceral mesoderm comprises metameric clusters of cells in the trunk, as well as a population of cells at the tail end of the embryo (caudal visceral mesoderm). In the trunk, two populations of myoblasts (founder myoblasts and fusion myoblasts) migrate to the midgut endoderm and then fuse to form the circular fibers. Longitudinal visceral muscles arise from the caudal visceral mesoderm from where they migrate anteriorly along the entire length of the gut (Campos-Ortega and Hartenstein, 1997; Martin et al., 2001). The cell-cell interactions controlling the specification of founder cells and fusion competent cells, as well as the fusion of these cell types, are similar to those described for the development of the somatic body wall muscle in *Drosophila* larvae, but also show some significant different features (Martin et al., 2001; Schröter et al., 2006; Rudolf et al., 2014).

In contrast to the well described embryonic development of the larval visceral muscle, few studies have been conducted that focus on the postembryonic events shaping the adult visceral muscle. During metamorphosis, the larval gut is replaced by an adult gut. The epithelium of the foregut, midgut, ureter and hindgut forms from undifferentiated, proliferatory progenitor cells (reviewed in Hartenstein and Chipman, 2016; Fig. 1A). This is similar to the adult epidermis and associated somatic musculature, which is also generated

de novo from populations of undifferentiated progenitor cells forming the imaginal discs and other cell clusters attached to the peripheral nerves (Bate et al., 1991; Figeac et al., 2010). By contrast, the adult visceral musculature appears to descend from larval visceral fibers that persist throughout metamorphosis. Using a Gal4/UAS transplant system, Klapper et al. (2000; 2002) generated labeled clones of visceral muscle in the larva and could show that these same cells made the transition into the adult gut. The same authors studied the metamorphosis of longitudinal fibers during pupal stages. They observed that at about 4 hr after puparium formation (APF) the longitudinal muscles begin to contract to the anterior and posterior regions of the midgut. At around 40 hrs muscles re-extend over the middle parts of the midgut. These findings indicate that longitudinal visceral muscle cells of the larval gut undergo a process of de-differentiation and then redifferentiated into adult muscle fibers (Fig. 1A). It is not known whether circular fibers, which constitute the majority of visceral muscle of the adult gut, form in a similar manner.

In the present study we used a combination of different approaches, including immunohistochemistry, lineage tracing and clonal analysis, and electron microscopy, to (1) confirm that larval visceral muscles persist into the adult; (2) establish the cellular mechanism by which the larval muscle metamorphoses into the adult; (3) study the relationship between the persisting visceral muscle layer and the enclosed enterocyte epithelium, which forms de novo from populations of undifferentiated progenitor cells. Previous studies had shown that the larval midgut epithelium contracts rapidly during the early hours of the pupal phase and eventually undergoes programmed cell death (Denton et al., 2009; 2010); the adult midgut epithelium (as well as a transient pupal midgut layer) forms by the rapid expansion and merger of adult midgut progenitors (AMPs) (Takashima et al., 2011a). Prior to metamorphosis, these cells form proliferating clusters of mesenchymal cells located in between the basal surface of the epithelium and surrounding muscle layer. At the onset of metamorphosis, concomitant with the contraction of larval enterocytes, AMPs undergo a rapid mesenchymal-to-epithelial transition to form the adult and pupal enterocyte layers (Takashima et al., 2011a; 2016). The epithelial layer of the hindgut and foregut is also replaced by a new set of adult cells. In contrast to the midgut, progenitors of the adult foregut and hindgut are integrated in the larval epithelium, where they form narrow, cylindrical domains at the boundaries between foregut/midgut, and hindgut/midgut, respectively (Singh et al., 2011; Takashima et al., 2008; 2013). The process by which progenitors of the adult foregut and hindgut proliferate, spread out to replace the larval enterocytes, and become ensheathed by visceral muscles has not been documented previously, and will be analyzed in the present study.

The final goal addressed in this work is to examine the role of the transforming visceral muscle layer on the emergence of intestinal stem cells (ISCs) in the pupal gut. Whereas the majority of adult gut progenitors differentiate into adult enterocytes during the early pupal stage, a subset remains undifferentiated and continues to proliferate throughout pupal stages and adulthood (Takashima et al., 2011b; 2016; Fig. 1A). In the adult midgut, the self-renewing activity and pattern of proliferation of ISCs is under the control of multiple signaling pathways, including Notch/Delta (Ohlstein and Spradling, 2006; Michelli and Perrimon, 2006), Jak/Stat (Beebe et al., 2010), EGF (Jiang and Edgar, 2009; Xu et al., 2011) and Wg (Lin et al., 2008; Xu et al., 2011). Similarly, hindgut ISCs, forming a continuous

belt at the anterior boundary of the hindgut (hindgut proliferation zone, HPZ; Fig. 1G) are under the control of Wg signaling and also express Stat, and their differentiation is mediated via Hh signaling (Takashima et al., 2008). During these signaling interactions, the (adult) visceral muscle layer appears to act as a "global niche" environment, supplying ligands like Wg and Vein. Given this role of the adult visceral musculature, and the fact that visceral muscle cells are continuously present, we speculated that signals from the metamorphosing musculature might also play a role in the formation of ISCs in the pupal gut, and undertook a study where visceral muscle was ablated from early pupal stages onward. As a result of this manipulation, both morphogenesis of the intestinal epithelium and the proliferation pattern of presumptive ISCs showed severe abnormalities, attesting to the role of visceral musculature in gut development.

MATERIALS AND METHODS

Fly stocks and maintenance

Fly lines used in this study were: *24B(How)-Gal4*, *tub-Gal80^{ts}*, *UAS-myr-mRFP*, *UAS-mCD8GFP*, *UAS-flp, Act5C promoter-FRT-phl[+]-FRT-lacZ.nls* (*Act5C >stop>lacZ*) (all provided by the Bloomington Stock Center), *esg-Gal4* (the National Institute of Genetics, Mishima, Japan), *UAS-hid UAS-rpr*, *10Xstat92E-GFP* (Bach et al., 2007), *ZCL1973X* (*Trol-GFP*) (Kelso et al., 2004), *wg-lacZ* (Struhl and Basler, 1993), *esg-GFP* (*YB0232*) (Kelso et al., 2004), y w hsFLP UAS-GFP (w+); tub>GAL80 y+>GAL4/SM5^TM6B (kindly provided by Dr. U. Banerjee). Flies were maintained with normal fly food at room temperature or in incubators set at 25°C or 18°C. In some experimental conditions, flies were transferred to the temperature at 29°C to suppress the function of *Gal80^{ts}*.

Immunohistochemistry

Antibody staining was performed as described previously (Takashima et al., 2011b). Shortly, dissected gut was fixed by 4% formaldehyde diluted with PBS-Tween (PBS containing 0.1% Tween20). After washing with PBS-Tween, gut samples were incubated with primary antibody for overnight at 4°C. The unbound antibody was washed out with PBT then the samples were incubated with secondary antibody labeled with fluorescent dye for overnight at 4°C. After washing, samples were stained with TOTO-3 or TOPRO-3 (Life Technologies, Carlsbad, CA) nuclear dye (1:1000 dilution in Vectashield) while mounting in Vectashield mounting medium (Vector Laboratories, Burlingame, CA). Throughout the procedure samples were kept in a tube placed on ice to prevent sample degradation. Antibodies used were (dilutions in parentheses): mouse antibodies against armadillo (arm, 1:10), prospero (pros, 1:50), Mef2 (1:50) (all obtained from the Developmental Studies Hybridoma Bank, University of Iowa), Rhodamine Phalloidin (Phal 1:500) (Molecular Probes), β-galactosidase (β-gal, 1:100) (Promega, Madison, WI), Bromo-deoxyuridine (BrdU; Sigma, St Louis), goat secondary antibodies against mouse IgG labelled Alexa488 (1:100), mouse IgG Alexa 546 (1:300), rabbit IgG Alexa488 (1:100) (Life Technologies); and rabbit Cy3 (1:200) (Jackson Immunoresearch, West Grove, PA).

BrdU incorporation assay

Labeling proliferative cells with BrdU was performed by injecting BrdU solution into pupa. After the pupal case was removed, the animal was injected with 20microL to 30microL of BrdU solution (approx. 1mg/mL; saturated in distilled water; Sigma, St Louis). After a given time interval, guts were dissected and fixed, treated with 2N HCl for 30 min on ice, and then processed for antibody staining.

Lineage trace experiments

To trace the lineage of pISCs in normal condition, flies with genotype of *tub-Gal80^{ts}/+; UAS-flp; Act5C>stop>lacZ/24B(How)-Gal4* were used. In the case of the tracing lineage with a gene over-expression or down-regulation, one of the wild-type chromosomes (indicated as "+") was replaced with an UAS-harboring chromosome by crossing. L3 Larvae raised at 18°C were transferred to 29°C to inactivate the Gal80^{ts} repressor resulting in an elimination of "Stop cassette" on *Act5C>stop>lacZ* transgene by an UAS-driven flipase to permanently label the cells of the visceral muscle lineage until P48 or adult stages.

Muscle ablation experiments

To effectively remove the visceral muscle during metamorphosis, female flies with genotypes *UAS-his UAS-rpr/(+ X-chromosome); tub-Gal80^{ts}/(+, stat92E-GFP, or esg-GFP); 24B(How)-Gal4/+* were used. Flies were grown at 18°C to either onset of puparium formation, 12h after puparium formation (APF), or 36h APF, then were transferred to 29°C for a duration of 48 hours to de-active the Gal80^{ts} repressor in order to allow for muscle deletion under the control of hid/rpr caspase. Controls for these experiments were grown under the same conditions, but were males without an affected X chromosome. When grown at 18°C growth developmental age is assumed to be about half that of normal development.

Cell counts

We consistently selected the posterior part of the midgut (next to the anterior hindgut) for cell counts. Preparations were recorded with an x40 oil lens, using the Zeiss LSM700 confocal microscope. Z-projections of 5–8 adjacent digital sections (2μm thickness) were generated, using the ImageJ (National Institute of Health) software package. From within these z-projections we counted manually all pISCs, enterocytes and endocrine cells in a field covered by an x40 objective at x2 zoom. We used the number of enterocytes as a reference point. Enterocytes do not increase in number during the pupal period, based on (1) clonal analysis showing that pISCs do not produce enterocytes in the pupa (Takashima et al., 2016); (2) temporally closely-spaced BrdU injections of pupae, indicating absence of cell division after during pupal development.

Clonal analysis

Single cell clones were generated by the flp-out technique (Golic and Lindquist, 1989), using flies with the genotype of y w hsFLP UAS-GFP (w+); tub>GAL80 y+>GAL4/ SM5^TM6B and applying a heat pulse at 37°C for 30 minutes to 1 hour at the puparium formation stage (white pupae). Heat-activated FLP will remove Gal80 in random cells (whose number depends on the duration of the pulse), and thereby induce GFP in these cells.

Transmission electron microscopy

Guts were fixed with 2.5% glutaraldehyde and 1% osmium tetroxyde and embedded in Epon resin following standard procedures optimized for pupal tissue (Takashima et al., 2011a). Ultra-thin sections were stained with uranyl acetate and lead citrate. JEOL 100CX transmission electron microscope was used for observation.

Results

Larval visceral muscles persist and metamorphose into visceral muscles of the adult

In the late larval gut, rhodamine-conjugated phalloidin (Phal), which labels myofibrils, shows the characteristic pattern of circular and longitudinal fibers introduced previously (Fig. 2A, B, C). Phal-positive myofibrils become irregular in shape and gradually disappear during the first day of metamorphosis (Fig. 2D, E, F) and are almost completely absent by 36h after hatching (P36; Fig. 2I–L). Phal-labeling of myofibrils reappears at P48 (Fig. 2M–O), and reveals the characteristic adult pattern of visceral muscle fibers by P72 (Fig. 2P, Q). The disintegration and later reappearance of myofibrils can be confirmed electron microscopically (see below).

The muscle specific driver line Held-out wing (How)-Gal4<Uas-mCD8::GFP labels the cytoplasm of visceral muscle, with a higher expression level in longitudinal fibers than circular fibers (Fig. 2A). Expression of this marker persists throughout pupal development in a dense layer of cells re-expressing the muscle determinant gene Mef2 (Fig. 2G–H′), demonstrating that visceral muscle cells are continuously present, even though they lose their myofibrils. This conclusion was supported by driving the lineage trace construct, *tub-Gal80^{ts}/+; UAS-flp; Act5C>stop>lacZ,* using How-Gal4. The stably expressed lacZ reporter was activated by a 24h heat pulse in the late larva. Subsequently animals were grown at 18°C until reaching the equivalent age of 48h APF, or eclosion. At both stages, lacZ-positive nuclei (green in Fig. 3A–B′) are present in circular and longitudinal fibers. The number and pattern of nuclei closely corresponds to the larval pattern. In particular, nuclei associated with circular fibers line up in two rows on each side of the midgut (Fig. 3B′; arrowheads). The lineage trace experiment confirms that the muscle cells present at the pupal and adult stage are the direct descendants of larval fibers.

Larval visceral fibers de-differentiate into secondary myoblasts during early metamorphosis

How-Gal4<Uas-mCD8::GFP expression in the 24h pupal gut reveals that longitudinal muscle syncytia morph into short, compact clusters containing 1–4 nuclei each, which we will call “secondary visceral myoblasts” in the following (Fig. 2D–E′). It is possible that cells within these clusters cells lose their syncytial configuration and become individualized, similar to the circular visceral muscle cells described below. In favor of this interpretation, longitudinal myoblasts spread out around P36 and, in many cases, appear as single cells that extend anteriorly and posteriorly directed processes (Fig. 2I). However, we cannot rule out that secondary longitudinal visceral myoblasts remain in syncytial contact via thin cytoplasmic bridges that evade detection by light microscopy. The dedifferentiation of longitudinal fibers that occurs during the first day of metamorphosis begins in the central

midgut and progresses from there to the anterior and posterior ends of the gut; in many specimens of P24 or P36, the central portion of the short midgut is completely devoid of longitudinal visceral fibers (Fig. 2D, I) This pattern of fiber concentration at the ends of the midgut maybe be due to loss muscle fiber connection to their attachment points, facilitated by a loss of the basement membrane (see below).

How-Gal4<UAS-mCD8::GFP expression in circular muscles reveals that these cells form a dense cellular layer around the enterocyte epithelium of the early pupal gut (Fig. 2J–L). Flp-out activated expression of GFP, following 45–60min long heat pulses applied to late wandering larvae allowed us to visualize individual muscle fibers (Fig. 4; number of recorded cases: 32). At P24 and P29, most labeled circular muscle cells are still bi-nucleated syncytial fibers (Fig. 4A–C). Syncytia are typically very thin and irregular in shape (Fig. 4B, C). At P29 and particularly at P48, many circular fibers have dissociated into rounded, mononucleated secondary myoblasts (Fig. 4D, D′; arrows). By P72, fusion of these cells into binucleated adult fibers has taken place; mononucleated cells were no longer recovered at this stage (Fig. 4E, F). Important to note is that the adult syncitia still surround one half of the gut perimeter, as in the larva (Fig. 4E, F).

BrdU pulses applied systematically at sequential time intervals during metamorphosis labeled the intestinal epithelial cells (see below), but not muscle nuclei, recognizable by their position peripheral to the intestinal epithelium (Fig. 5H, H′; arrow). Our finding, which matches previously reported counts of longitudinal visceral muscle nuclei (~500–530 muscle nuclei in the late larva and the adult; Klapper et al., 2000) indicates that secondary myoblasts proliferate little, if any, during gut metamorphosis.

The basement membrane surrounding the adult visceral muscle develops de novo during metamorphosis

We next analyzed the changes exhibited by the basement membranes surrounding visceral muscles during metamorphosis. To this end, we used a protein trap line for the *Drosophila* homologue of the heparan sulfate proteoglycan Perlecan, Terribly reduced optic lobes (Trol), in conjunction with transmission electron microscopy. Trol-GFP had been shown in previous work (e.g., Grigorian et al., 2013) to be expressed in all basement membranes of the larva and adult. In the late larva and early (0–6h) pupa, expression of a Trol-GFP reporter appears as a continuous layer completely surrounding each circular and longitudinal visceral muscle fiber (Fig. 6A–D′). Electron microscopically, the electron dense basement membrane appears as a layer of 60–120nm thickness that surrounds visceral muscle (Fig. 7A′, B′).

During the first day following puparium formation, prior to the stage at which myofibrils disintegrate and fibers dissociate (see above), the Trol-GFP expression becomes punctate (Fig. 6E–J′). By P24, basement membranes have mostly disappeared (Fig. 6K–M′). What remains of Trol-GFP-positive material appears as globular particles located basally to the visceral muscle in the midgut and the hindgut, or is contained within macrophages which populate the surface of the early pupal gut (Fig. 6K, L′, M′; arrowheads; Fig. 7C). Interestingly, in the ureter and proximal Malpighian tubules, which are largely retained from larval to adult stage (Singh et al., 2007; Takashima et al., 2013), visceral muscle surrounded by Trol-GFP-positive basement membranes persist as a continuous layer (Fig. 6K). Electron

microscopy confirms that basement membranes are absent from the P20 gut; the basal cell membrane of the enterocyte epithelium directly contacts membranes of secondary myoblasts (Fig. 7D′, arrows). Likewise, myofibrils are scarce (Fig. 7D′, E′) and do not form the regular hexagonal arrays characteristic of the myofibrils seen in the larval or adult visceral muscle (Fig. 7A′).

Basement membranes are built up again around the stage when secondary myoblasts fuse into adult visceral muscle and myofibrils reappear. At P48, a thin (10–40nm), relatively light layer of floccular material surrounds the muscle, separating it from the intestinal epithelium (Fig. 7E′ arrowheads). At P72, the strong Trol-GFP-positive layers around muscle fibers seen in the confocal microscope (Fig. 6N–P′) parallels the electron microscopic image, which shows an ECM dense basement membrane of >50nm diameter (Fig. 7F,F′). Our findings indicate that the basement membranes separating visceral muscle cells from the adjacent intestinal epithelium and surrounding hemolymph completely melt down and are then rebuild during metamorphosis.

Metamorphosis of the hindgut and midgut proceeds within the persisting sheath of secondary myoblasts

Our findings presented above demonstrate that the visceral muscle, including both circular and longitudinal fibers, persist through metamorphosis, even though the attachment of fibers and the syncytial structure of fibers transiently breaks down. Within the “sleeve” formed by the muscle cells, the intestinal epithelium changes from its larval to adult configuration. In contrast to what we see in the visceral muscle, larval intestinal cells undergo programmed cell death, and are replaced by a new set of adult specific cells which descend from the adult gut progenitors. In the early pupal midgut (P0–P6), whose development has been described in detail by Takashima et al. (2011a; 2016), adult progenitors undergo a mesenchymal to epithelial transition, forming a layer of adult polarized epithelial cells that surround the degenerating larval gut. Between P6 and P24, the midgut contracts in length and expands in diameter, forming a spindle-shaped structure enclosing the compacted degenerating larval and pupal midgut (“yellow body”; compare Figs. 8A and 8B; Fig. 8N provides a time line listing the major morphogenetic events shaping midgut and hindgut). After 36h of pupal development, the adult midgut epithelium extends into an elongated, coiled tube. This process, which is accompanied by convergence-extension movement of the epithelial cells, coincides temporally with the reconstitution of adult visceral muscle fibers, as described above (Fig. 8C, N).

The adult hindgut arises from intestinal progenitors which form a narrow cylindrical domain, the HPZ, at the boundary between midgut and hindgut (Takashima et al., 2008; Fig. 8D). This domain spreads posteriorly, pushing the larval epithelium backwards. The smaller cell size of the adult hindgut precursors, compared to the large, polyploidy larval enterocytes, marks a clear boundary between the extending adult hindgut and the retreating larval hindgut (Fig. 8I, arrow). During the first day of pupal development, spreading of the HPZ is slow. At P12, the pupal hindgut, unlike the adjacent midgut, is still formed by larval enterocytes surrounded by a relatively intact layer of circular muscles (Fig. 8D–G). At P24, the HPZ has expanded to about 25% length of the pupal hindgut; the retracting larval

hindgut shows irregularly shaped enterocytes flanked by macrophages (Fig. 8H, I), a clear sign of the impending programmed cell death. A phase of rapid expansion between 24 and 36h APF propels the adult hindgut posteriorly, and by P48 only adult hindgut cells, posteriorly contacted by the rectum which develops from the genital imaginal disc, remain (Fig. 8J–N). Unlike the midgut, the larval hindgut is not taken up into the lumen of the newly formed adult hindgut. Instead, larval hindgut cells appear to dissociate and are taken up by surrounding macrophages.

In order to determine when cells of the evolving hindgut proliferate, we performed BrdU incorporation assays at varying lengths during metamorphosis. BrdU pulses in the hindgut in the pupa suggest only one doubling of cells in early hindgut metamorphosis, which occurs between the late larval stage and P6 (Fig. 5A–C). Shortly before the expansion of the adult hindgut another phase of global BrdU incorporation can be observed (Fig. 5D–H). We surmise that this phase of DNA synthesis corresponds to endoreplication, based on the fact that hindgut cells increase in size, and that the number of adult cells is only about twice that of larval cells (Fox et al., 2009). BrdU incorporation in the hindgut ceases after the full extension of the adult hindgut (Fig. 5I, J).

In the midgut, presumptive stem cells are ‘set aside’ early in metamorphosis, at a time when AMPs spread out and merge into the adult midgut epithelium (Takashima et al., 2016). How does the stem cell zone that forms the anterior boundary of the adult hindgut develop? The HPZ of the larval hindgut is marked by the expression of high levels of Stat92E-GFP (Takashima et al., 2008; Fig. 9A). A row of cells at the anterior boundary of the HPZ expresses Wg, a signal required to maintain hindgut progenitor cells in an undifferentiated, dividing state (Fig. 9A′). The same configuration of Wg and Stat is seen in the HPZ of the adult hindgut, where cells continue to divide, albeit at a much lower rate than in the midgut (Takashima et al., 2008; Fox et al., 2009). To investigate the emergence of the adult hindgut stem cells we labeled pupal hindgut preparations with Stat92E-GFP and a Wg-lacZ reporter. During the first day of metamorphosis, as the HPZ starts to expand posteriorly, the expression level of both markers decreases (Fig. 9C). At this stage, the larval HPZ undergoes its transition into the adult hindgut epithelium (“HPZ>ahg” in Fig. 9C–D′). In addition, the most anterior cells of the larval HPZ, which remain positive for Stat (Fig. 9B, B′, C), as well as Wg-lacZ (Fig. 9D,D′), expand anteriorly, to become the “plug” (pl in Fig. 9B′, C, D′) that later gives rise to the posterior segment of the adult midgut (Takashima et al., 2013; “mg_{po}” in Fig. 9E–H′; see also Fig. 1A). A distinct HPZ, which would differ in cell size, proliferation, or expression of genetic markers is absent in the early pupa: all cells of the former HPZ (the “HPZ>ahg” in Fig. 9C–D′) display the same phenotype. The adult HPZ makes its appearance around P48, and is marked by a new phase of expression of Stat and Wg. Stat expression is restricted to the anterior 5–7 rows of cells of the HPZ, which become the so called spindle cell zone of the adult HPZ (“aHPZ” in Fig. 9E,G). Wg-lacZ reappears at the midgut-hindgut boundary at P48 (Fig. 9F–F″). Initially, this new Wg-lacZ signal is localized in two rows of midgut circular muscle (arrowhead in Fig. 9F′, F″) directly adjacent to, but not overlapping with the Wg-lacZ signal present in the anterior HPZ (arrow in Fig. 9F′,F″). By P72, a bright Wg-lacZ signal is present in both the HPZ and the two circular muscle cells at the midgut/hindgut boundary (Fig. 8H–H″). These Wg-lacZ signals

are maintained in the adult. In the epithelium, the Wg-lacZ domain becomes more restricted to one cell row right at the boundary of the HPZ.

The effect of visceral muscle on the development of the hindgut and midgut

We speculated that the visceral muscle layer, which persists throughout metamorphosis, may play multiple roles with regards to the formation of the gut epithelium. First, the muscle layer may be important for normal gut morphogenesis, in particular the convergent extension resulting in the elongated tubular structure of the gut; secondly, given the known role of the adult visceral muscle as a “global niche” involved in the control of ISC proliferation, visceral muscle fibers could be important in the patterning and proliferation of presumptive ISCs in the pupal gut. To address these hypotheses, we ablated the visceral musculature, using a tub-Gal80ts How-Gal4 driven activation of UAS-hid/UAS-rpr, proteins known to promote caspase mediated apoptosis, and evaluated the structure of the gut at a time point corresponding to the normal time of eclosion (96–100h APF). The effectiveness of muscle ablation was monitored by labeling with phalloidin.

In both midgut and hindgut, visceral muscle ablation stunts morphogenesis and impacts the emergence of pISCs. Thus, following ablation between 12 and 60h, or 36 and 84h, the adult midgut epithelium forms a continuous layer and expands, but retains its short, wide configuration that is seen in early control midguts. The subsequent extension towards an elongated tube that is typical for the late pupal wild-type midgut fails to occur (Fig. 10A, B), which is likely due to either a lack of signaling or scaffolding functionality of the muscle. In the hindgut, ablation of visceral muscle at around 12h APF abrogates extension of the HPZ and removal of the larval hindgut. The larval hindgut persists, even though increased amount of macrophages and signs of apoptosis exist among its cells. (Fig. 10D,E arrow). At the same time, the HPZ often bulges outward, forming a short, wide structure co-existing with a persisting larval hindgut (Fig. 10F). Muscle ablation at later stages (between 36hrs and 84hrs) were correlated with more extended HPZs and the disappearance of larval hindgut cells; still, the emerging hindgut is considerably shorter than that of control animals (not shown).

There is also a significant effect of muscle ablation on the development of presumptive midgut ISCs. During the course of normal development, these cells can be clearly recognized shortly after puparium formation; they undergo three waves of division at approximately 24h APF, 48h APF, and in the late pupa (Takashima et al., 2016). Ablating visceral muscle (heat pulse 12–60 APF) significantly reduced the number of pISCs, which were labeled by their expression of the reporter Esg-GFP (Fig. 11A–B′). The ratio of pISCs to enterocytes (whose number remains constant from 12h APF to eclosion; Takashima et al., 2016) amounts to 21.0% (s.d.=5.2%) in the control, versus 7.0% (s.d.= 1.8%; n=4) in experimental animals. Similarly, following muscle ablation, the number of Prospero-positive endocrine cells is reduced (control: 12.9%, s.d.=2.5%; n=4; experimental: 3.3%, s.d.=0.9%; n=4), indicating that the muscle plays a roll not only in pISC maintenance, but also their development (Fig. 11C,D).

The development of the hindgut proliferation zone also showed abnormalities in the absence of pupal visceral muscle. As described above, in control animals, the renewed expression of

the marker Stat that occurs around 48 APF expression is restricted to a narrow domain bordering the midgut hindgut boundary (Fig. 11E). Following the induction of visceral muscle cell death by a 24–60h APF pulse, Stat expression in the newly emerging HPZ remains at a relatively low levels and occupies a much wider zone than in the control (Fig. 11E,F arrowheads). We were not able to ascertain definitive changes in the number of HPZ cells that continue to proliferate, but we speculate that, similar to midgut ISCs, hindgut ISCs may be lacking or reduced in number in the absence of surrounding visceral muscle.

Our findings demonstrate that the presence of visceral muscle is a prerequisite for normal intestinal epithelial morphogenesis. Cell re-arrangements leading to gut elongation do not take place normally if visceral fibers are ablated; in addition, the maintenance and/or re-appearance of proliferating intestinal stem cells is affected by visceral muscle loss.

Discussion

Developmental dynamics of the visceral and somatic musculature

The structure of the *Drosophila* visceral muscle system, consisting of an interwoven network of circular and longitudinal muscle, formed by syncytial, striated fibers, is representative for insects in general. However, information concerning the development and metamorphosis of visceral muscle is scarce in the previous literature. The finding that in *Drosophila*, larval visceral muscle persists into the adult, reported by Klapper (2000) and confirmed and extended in the present study, appears to apply to other insect taxa. For example, in the mosquito *Aedes aegypti* midgut, muscle fibers persist but undergo a transient phase of atrophy (Bernick et al., 2007; 2008), whereby myofibrils degenerate, similar to the situation in *Drosophila* described here. Thus, in the 6h–21h (approximately 20–80% of the duration of metamorphosis) pupal midgut, muscle fibers visualized by scanning electron microscopy appear flattened in comparison to earlier pupa stages or the adult; at the same time, myofibrils shown by TEM, disappear. It was not reported in this study whether any syncytial fibers dissociated into individual cells.

The postembryonic development of visceral muscle in *Drosophila* and other holometabolous insects appears to differ fundamentally from somatic muscle in that it does not involve undifferentiated progenitors from which a new set of adult muscles is generated. Thus, for somatic muscle, a pool of progenitors (progenitors of the adult somatic muscles or ASMPs) split from the mesoderm during early embryogenesis (Bate et al., 1991). These cells maintain high levels of muscle-specific transcription factors, like Twist (Twi). Attached to the imaginal discs and peripheral nerves, ASMPs are mitotically quiescent in the embryo, and proliferate rapidly in the late larva and pupa. During metamorphosis, ASMPs fuse in a process similar to that described for the embryo (Roy and VijayRaghavan, 1999). The pattern of larval muscles prior to their demise serves as a scaffold around which ASMPs spread and then fuse into syncytia. In some cases, notably the indirect flight muscles, larval muscles are incorporated into the adult myotubes.

Similar to the postembryonic somatic muscle in *Drosophila*, vertebrate skeletal muscle is also associated with a pool of undifferentiated stem cells, called satellite cells. Satellite cells are located within in the basement membrane surrounding the differentiated muscle fibers.

Satellite cells are maintained by signals and structural components of the basement membrane, which serves as their niche (Thomas et al., 2015). It has been shown for several vertebrate models that satellite cells, just like the regular muscle fibers, derive from the myotome that forms part of the early embryonic somite (Relaix et al., 2005). During the course of embryogenesis, most cells of the myotome spread out and assemble into the muscles attached to the axial and appendicular skeleton. A subset of cells maintain expression markers of undifferentiated myoblasts, such as Pax7, and become satellite cells. In the adult animal, satellite cells respond in a regenerative capacity to muscle damage (Lepper et al. 2011), and to stress caused by increased physical activity (Kadi et al. 2004).

Aside from the pool of undifferentiated satellite cells, myocytes themselves can also proliferate to produce new muscle fibers. Thus, skeletal myocytes have the capacity to dedifferentiate into single celled myocytes and redifferentiate in reaction to myotube damage. In once case Mu et al. (2011) tested this hypothesis by inducing lacerations to muscle in mice which had muscle derived cells (MDCs) either expressing ubiquitous Cre-recombinase or LoxP sites flanking a stop codon followed by a β-galactosidase gene. Muscle fibers formed by a fusion of these two MDC types were identified by their expression of B-galactosidase. After muscle injury, mononuclear β-gal positive myocytes were formed from these fibers. When isolated and cultured, the mononuclear cells proliferated formed syncytial myotubes (Mu et al., 2011). This phenomenon resembles the formation of “secondary myoblasts” in the metamorphosing *Drosophila* visceral musculature, and could involve related molecular mechanisms.

Visceral muscle in vertebrates has diverse origins; intestinal muscle fibers are derived from the splanchnopleural layer surrounding the endoderm of the early embryo, vascular muscle progenitors form part of the neural crest, or develop from mesenchymal cells surrounding the blood vessels. Vertebrate visceral muscle differs from its insect counterpart by possessing smooth (non-striated) myofibrils, and forming mononuclear fibers, rather than syncytia. For later visceral muscle growth and regeneration, a number of different mechanisms and stem cell systems have been described. It has long been thought that many types of smooth muscle, in particular vascular smooth muscle cells, dedifferentiate, proliferate, and redifferentiate in response to disease and damage (Owens, 1995; Layne et al., 2002). There have been studies to show the potential for these cells to be induced into dedifferentiation *in vitro* (Lehti et al., 2009). Recently it was found that undifferentiated multipotent mesenchymal stem cells (MVSCs) in the media layer of the vessel wall also play a role in vascular muscle growth and regeneration (Tang et al., 2012). MVSCs, confirmed via lineage trace analysis, were able to proliferate and differentiate in response to vascular injury. SM-MHC-/Ki67+ cells isolated from the tunica media and left in culture after a 30 day period showed morphological changes as well as increased expression of smooth muscle actin (SMA) and calponin-1 (CNN-1) which are highly expressed in mature smooth muscle cells. Similar to vascular smooth muscles, the myometrium also contains a pool of undifferentiated, proliferating cells located at the periphery of smooth muscle bundles. Though their origins are not well defined, these cells are hypothesized to be the regenerative satellite cells for repairing myometrial wall damage (Szotek et al., 2007, Arango et al., 2005).

In conclusion, in vertebrates, both somatic and visceral muscles use undifferentiated stems cells, as well as dedifferentiation/remodeling of existing myocytes for postembryonic growth and tissue regeneration. The dedifferentiation process we here describe for the *Drosophila* visceral musculature might well be controlled by the same molecular networks that guide muscle regeneration in vertebrates, and could therefore constitute a useful model for further analysis of these networks.

The effect of visceral musculature on intestinal morphogenesis and stem cell proliferation

The endodermally derived intestinal epithelium and the surrounding visceral muscle layer are in close contact to each other from early embryogenesis onward, and continuously exchange signals guiding each others development. One of the first steps of *Drosophila* gut development that depends on the contact with visceral mesoderm is the mesenchymal-epithelial transition of endodermal cells resulting in the midgut epithelium (Tepass and Hartenstein, 1994). Genetic ablation of visceral mesoderm causes the endoderm to remain as a cluster of non-polarized, mesenchymal cells. Subsequently, the regionalization of the midgut into discrete, functionally different domains along the antero-posterior axis depends on interactions between visceral mesoderm and endoderm. The mesoderm expresses four Hox genes, Scr, Antp, Ubx, and Abd-A, in an anterior to posterior order. Each of these is important for the differentiation of the endodermal cells flanking its expression domain in the mesoderm. For example, loss of Scr results in the absence of gastric caeca that normally invaginate from the first chamber midgut chamber. Loss of AbdA and Ubx cause the absence of copper cells from the middle part of the midgut. Here, a Wg signal, activated by AbdA/Ubx in the visceral mesoderm, triggers expression of Labial in the adjacent endoderm, which again is required for copper cell development (Bienz, 1994).

As shown in the present paper, interaction between visceral musculature and intestinal epithelium continue throughout metamorphosis. Visceral fibers are required for the cell rearrangement resulting in the elongation of midgut and hindgut respectively. In case of the hindgut, visceral fibers are instrumental in the destruction of larval enterocytes. We hypothesize that the foregut, which develops in a similar way as the hindgut (expanding proliferation zone of adult progenitors expanding and replacing degenerating larval foregut; Singh et al., 2011) will also depend on visceral muscle for its development. It is currently unknown which signals and structural molecules are active in mediating the interaction between muscle layer and enterocytes. It stands to reason that the extracellular matrix, whose reconstitution takes place during the second half of metamorphosis when also enterocytes rearrange and the gut lengthens, plays an important role.

The visceral muscle layer also plays a role during the development of intestinal stem cells. In the midgut, presumptive ISCs (pISCs) emerge shortly after the onset of metamorphosis and undergo three waves of division during metamorphosis (Takashima et al., 2016). During the first wave, they divide symmetrically, merely doubling in number. From the second wave onward, endocrine cells start to appear among the progeny of pISCs, but no enterocytes; these are specified for the first after eclosion (Takashima et al., 2016). Our present study shows that ablation of visceral muscle cells during metamorphosis affects the proliferation rate of pISCs, which is not unexpected given the function of visceral muscle-derived signals

in the adult (an experiment of ablating visceral muscle in the adult to study abnormalities in the remaining gut epithelium has not been reported yet). Our findings also suggest that the reorganization of the musculature during metamorphosis may explain the changing lineage of pISCs at different stages that we recently described (Takashima et al., 2016). Previous published findings had identified the visceral musculature of the adult midgut as a major source of “niche signals”: Wingless and EGFR ligands (Lin et al., 2008; Jiang and Edgar, 2009; 2011; Xu et al., 2011; Biteau and Jasper, 2011) are expressed in the visceral musculature. In addition, differentiated enterocytes, as well as endocrine cells may emit signals that modulate the proliferation of ISCs (Buchon et al., 2010; Xu et al., 2011; Scopelliti et al., 2014; Biteau and Jasper, 2014). Our finding that visceral muscle ablation in pupae affects the pISC fate, and when depleted also cause a reduction of endocrine cell formation from pISCs, support the idea of a diffuse “visceral muscle niche” acting upon the pISCs. This then would represent a straightforward explanation for the changing behavior of pISCs during pupal development: Visceral muscle cells de-differentiate and then re-differentiate during metamorphosis, as shown by our findings. We speculate that production/presentation of the “niche signal” acting upon pISCs diminishes during this time of muscle involution. From about 36 hours APF onward the muscle is rebuilt into its adult shape, and that may also be accompanied by niche signal re-appearance. Thus, from about 48 hours APF onward, signals stimulating *pros* expression cause the appearance of endocrine cells. Other unknown (but also possibly muscle related) signals responsible for the levels of N activity that drives ISCs towards the enterocyte pathway only appear around the time of eclosion.

Though the visceral muscle is known to play an important role in midgut maintenance, little is known about its role in maintenance of the hindgut. Our data show that the adult hindgut develops from the HPZ, a narrow cylinder of progenitors located at the midgut-hindgut boundary. Following the onset of metamorphosis, these cells undergo one more round of division, then protrude posteriorly, “pushing” the degenerating larval hindgut layer ahead of them, and zippering up with the newly formed adult rectum (which is derived from a growth zone separate from the HPZ) by 48h APF. At around the same stage, an adult HPZ is re-constituted at the midgut-hindgut boundary. Like the larval HPZ, its adult counterpart is characterized by a narrow, discrete band of high levels of Stat expression, anteriorly flanked by a row of Wg-positive cells (Takashima et al., 2008). The appearance of these markers coincides with the re-differentiation of visceral muscle. Ablation of visceral muscle, while not abolishing Stat and Wg at the hindgut-midgut boundary, results in a widening of their domain and a lower expression level of these factors.

Reciprocal signals exchanged between endoderm and visceral mesoderm also orchestrate vertebrate gut development (McLin et al., 2009). In the early embryo, the endoderm signals to the visceral mesoderm via Sonic hedgehog (Shh). In response to the Shh signal, visceral mesoderm cells express FoxF1/F2 transcription factors (Mahlapuu et al., 2001a/b), homolog of the fly gene biniou which also forms an essential part of the gene network required for visceral muscle specification and differentiation. Loss of FoxF1/F2 results in disorganized and undifferentiated smooth muscle cells. The FoxF proteins in turn activate the expression of Wnt and BMP proteins which signal back to the endodermal epithelium, where they are involved in ISC proliferation and enterocyte differentiation (Ormestad et al., 2006). The

mature vertebrate intestinal epithelium is composed of a heterogeneous community of cells. It comprises enterocytes, secretory goblet cells, endocrine cells, Paneth cells and intestinal stem cells (ISCs). The latter two types are located within the crypts; differentiated enterocytes and secretory cells populate the villi. The mesenchymal tissue bordering the epithelium includes smooth muscle cells as well as undifferentiated myo-fibroblasts. The latter cells are thought to form part of the niche environment that provides signals for the maintenance and proliferation of the ISCs (Yen and Wright, 2006; Scoville et al., 2008). In addition, the epithelial Paneth cells of the crypt are also implicated in the niche (Sato et al., 2011). Wnt signals, which are expressed by both the myofibroblasts and Paneth cells, provide signals for proliferation and self-renewal (Gregorieff et al., 2005; Sato et al., 2011).

In conclusion, visceral muscle of *Drosophila* and vertebrates alike represents an important source of signals controlling intestinal development, maintenance and regeneration. Many of the underlying regulatory gene networks appear to be highly conserved. The metamorphosing *Drosophila* gut encountered during the pupal stage of development in many ways resembles a rapidly regenerating tissue. The pupal stage offers the experimental advantage of immobility, where live recordings can be carried out through small windows cut into the relatively opaque outer cuticle (e.g., Ninov and Martin-Blanco, 2007; Zitserman and Roegiers, 2011). Most importantly, genetic manipulations which would be lethal in a freely moving (and feeding) larva or adult, are compatible with pupal survival. For example, pupae develop to the point of eclosion even after almost complete ablation of the hindgut epithelium (Takashima et al., 2008). As a result, a wide spectrum of phenotypes can be studied in the pupa, which would be difficult at other (postembryonic) stages. We therefore believe that the metamorphosing *Drosophila* gut presents a favorable model to make progress in analyzing the gene networks controlling intestinal development.

References

Arango NA, Szotek PP, Manganaro TF, Oliva E, Donahoe PK, Teixeira J. Conditional deletion of beta-catenin in the mesenchyme of the developing mouse uterus results in a switch to adipogenesis in the myometrium. Dev Biol. 2005; 288:276–283. [PubMed: 16256976]

Azpiazu N, Frasch M. tinman and bagpipe: two homeo box genes that determine cell fates in the dorsal mesoderm of Drosophila. Genes Dev. 1993; 7:1325–1340. [PubMed: 8101173]

Bach EA, Ekas LA, Ayala-Camargo A, Flaherty MS, Lee H, Perrimon N, Baeg GH. GFP reporters detect the activation of the Drosophila JAK/STAT pathway in vivo. Gene Expr Patterns. 2007; 7:323–331. [PubMed: 17008134]

Bate M, Rushton E, Currie DA. Cells with persistent *twist* expression are the embryonic precursors of adult muscles in Drosophila. Development. 1991; 113:79–89. [PubMed: 1765010]

Bate, M. The mesoderm and its derivatives. In: Bate, M.; Martinez-Arias, A., editors. The development of Drosophila melanogaster. Cold Spring Habor Laboratory Press; Plainview: 1993. p. 941-1012.

Beebe K, Lee WC, Micchelli CA. JAK/STAT signaling coordinates stem cell proliferation and multilineage differentiation in the Drosophila intestinal stem cell lineage. Dev Biol. 2010; 338:28–37. [PubMed: 19896937]

Bernick EP, Moffett SB, Moffett DF. Organization, ultrastructure, and development of midgut visceral muscle in larval *Aedes aegypti*. Tissue Cell. 2007; 39:277–92. [PubMed: 17675126]

Bernick EP, Moffett SB, Moffett DF. Ultrastructure and morphology of midgut visceral muscle in early pupal Aedes aegypti mosquitoes. Tissue Cell. 2008; 40:127–141. [PubMed: 18160088]

Bienz M. Homeotic genes and positional signaling in the Drosophila viscera. Trends Genet. 1994; 10:22–26. [PubMed: 7908470]

Biteau B, Jasper H. EGF signaling regulates the proliferation of intestinal stem cells in Drosophila. Development. 2011; 138:1045–1055. [PubMed: 21307097]

Biteau B, Jasper H. Slit/Robo signaling regulates cell fate decisions in the intestinal stem cell lineage of Drosophila. Cell Rep. 2014; 7:1867–1875. [PubMed: 24931602]

Buchon N, Broderick NA, Kuraishi T, Lemaitre B. Drosophila EGFR pathway coordinates stem cell proliferation and gut remodeling following infection. BMC Biol. 2010; 8:152. [PubMed: 21176204]

Campos-Ortega, JA.; Hartenstein, V. The Embryonic Development of Drosophila melanogaster. 2. Springer; 1997.

Dhanyasi N, Segal D, Shimoni E, Shinder V, Shilo BZ, VijayRaghavan K, Schejter ED. Surface apposition and multiple cell contacts promote myoblast fusion in Drosophila flight muscles. J Cell Biol. 2015; 211:191–203. [PubMed: 26459604]

Denton D, Shravage B, Simin R, Mills K, Berry DL, Baehrecke EH, Kumar S. Autophagy, not apoptosis, is essential for midgut cell death in Drosophila. Curr Biol. 2009; 19:1741–1746. [PubMed: 19818615]

Denton D, Shravage B, Simin R, Baehrecke EH, Kumar S. Larval midgut destruction in Drosophila: not dependent on caspases but suppressed by the loss of autophagy. Autophagy. 2010; 6:163–165. [PubMed: 20009534]

Figeac N, Jagla T, Aradhya R, Da Ponte JP, Jagla K. Drosophila adult muscle precursors form a network of interconnected cells and are specified by the rhomboid-triggered EGF pathway. Development. 2010; 137:1965–1973. [PubMed: 20463031]

Fox DT, Spradling AC. The Drosophila hindgut lacks constitutively active adult stem cells but proliferates in response to tissue damage. Cell Stem Cell. 2009; 5:290–297. [PubMed: 19699165]

Golic KG, Lindquist S. The FLP recombinase of yeast catalyzes site-specific recombinantion in the Drosophila genome. Cell. 1989; 59:499–509. [PubMed: 2509077]

Gregorieff A, Clevers H. Wnt signaling in the intestinal epithelium: from endoderm to cancer. Genes Dev. 2005; 19:877–890. [PubMed: 15833914]

Grigorian M, Liu T, Banerjee U, Hartenstein V. The proteoglycan Trol controls the architecture of the extracellular matrix and balances proliferation and differentiation of blood progenitors in the Drosophila lymph gland. Dev Biol. 2013; 384:301–312. [PubMed: 23510717]

Hartenstein, V. The muscle pattern in Drosophila. In: Sink, H., editor. Muscle Development in Drosophila. 2005.

Hartenstein, V.; Chipman, AD. Hexapoda: A Drosophila's View of Development. 2016.

Jiang H, Edgar BA. EGFR signaling regulates the proliferation of Drosophila adult midgut progenitors. Development. 2009; 136:483–493. [PubMed: 19141677]

Jiang H, Edgar BA. Intestinal stem cells in the adult Drosophila midgut. Exp Cell Res. 2011; 317:2780–2788. [PubMed: 21856297]

Kadi F, Schjerling P, Andersen LL, Charifi N, Madsen JL, Christensen LR, Andersen JL. The effects of heavy resistance training and detraining on satellite cells in human skeletal muscles. J Physiol. 2004; 558:1005–1012. [PubMed: 15218062]

Kelso RJ, Buszczak M, Quiñones AT, Castiblanco C, Mazzalupo S, Cooley L. Flytrap, a database documenting a GFP protein-trap insertion screen in Drosophila melanogaster. Nucleic Acids Res. 2004; 32(Database issue):D418–20. [PubMed: 14681446]

Klapper R. The longitudinal visceral musculature of Drosophila melanogaster persists through metamorphosis. Mech Dev. 2000; 95:47–54. [PubMed: 10906449]

Klapper R, Heuser S, Strasser T, Janning W. A new approach reveals syncytia within the visceral musculature of Drosophila melanogaster. Development. 2001; 128:2517–2524. [PubMed: 11493568]

Layne MD, Yet SF, Maemura K, Hsieh CM, Liu X, Ith B, Lee ME, Perrella MA. Characterization of the mouse aortic carboxypeptidase-like protein promoter reveals activity in differentiated and dedifferentiated vascular smooth muscle cells. Circ Res. 2002; 90:728–736. [PubMed: 11934842]

Lee T, Luo L. Mosaic analysis with a repressible cell marker (MARCM) for Drosophila neural development. Trends Neurosci. 2001; 24:251–254. [PubMed: 11311363]

Lee HH, Norris A, Weiss JB, Frasch M. Jelly belly protein activates the receptor tyrosine kinase Alk to specify visceral muscle pioneers. Nature. 2003; 425:507–512. [PubMed: 14523446]

Lehti K, Rose NF, Valavaara S, Weiss SJ, Keski-Oja J. MT1-MMP promotes vascular smooth muscle dedifferentiation through LRP1 processing. J Cell Sci. 2009; 122:126–135. [PubMed: 19066283]

Lepper C, Partridge TA, Fan CM. An absolute requirement for Pax7-positive satellite cells in acute injury-induced skeletal muscle regeneration. Development. 2011; 138:3639–3646. [PubMed: 21828092]

Lin G, Xu N, Xi R. Paracrine Wingless signalling controls self-renewal of Drosophila intestinal stem cells. Nature. 2008; 455:1119–1123. [PubMed: 18806781]

Maggert K, Levine M, Frasch M. The somatic-visceral subdivision of the embryonic mesoderm is initiated by dorsal gradient thresholds in Drosophila. Development. 1995; 121:2107–2116. [PubMed: 7635056]

Mahlapuu M, Ormestad M, Enerbäck S, Carlsson P. The forkhead transcription factor Foxf1 is required for differentiation of extra-embryonic and lateral plate mesoderm. Development. 2001; 128:155–166. [PubMed: 11124112]

Mahlapuu M, Enerbäck S, Carlsson P. Haploinsufficiency of the forkhead gene Foxf1, a target for sonic hedgehog signaling, causes lung and foregut malformations. Development. 2001; 128:2397–2406. [PubMed: 11493558]

Martin BS, Ruiz-Gómez M, Landgraf M, Bate M. A distinct set of founders and fusion-competent myoblasts make visceral muscles in the Drosophila embryo. Development. 2001; 128:3331–3338. [PubMed: 11546749]

McLin VA, Henning SJ, Jamrich M. The role of the visceral mesoderm in the development of the gastrointestinal tract. Gastroenterology. 2009; 136:2074–2091. [PubMed: 19303014]

Micchelli CA, Perrimon N. Evidence that stem cells reside in the adult Drosophila midgut epithelium. Nature. 2006; 439:475–479. [PubMed: 16340959]

Mu X, Peng H, Pan H, Huard J, Li Y. Study of muscle cell dedifferentiation after skeletal muscle injury of mice with a Cre-Lox system. PLoS One. 2011; 6(2):e16699. [PubMed: 21304901]

Ninov N, Martín-Blanco E. Live imaging of epidermal morphogenesis during the development of the adult abdominal epidermis of Drosophila. Nat Protoc. 2007; 2:3074–3080. [PubMed: 18079706]

Ohlstein B, Spradling A. The adult Drosophila posterior midgut is maintained by pluripotent stem cells. Nature. 2006; 439:470–474. [PubMed: 16340960]

Ormestad M, Astorga J, Landgren H, Wang T, Johansson BR, Miura N, Carlsson P. Foxf1 and Foxf2 control murine gut development by limiting mesenchymal Wnt signaling and promoting extracellular matrix production. Development. 2006; 133:833–843. [PubMed: 16439479]

Owens GK. Regulation of differentiation of vascular smooth muscle cells. Physiol Rev. 1995; 75:487–517. [PubMed: 7624392]

Relaix F, Rocancourt D, Mansouri A, Buckingham M. A Pax3/Pax7-dependent population of skeletal muscle progenitor cells. Nature. 2005; 435:948–953. [PubMed: 15843801]

Roy S, VijayRaghavan K. Muscle pattern diversification in Drosophila: the story of imaginal myogenesis. Bioessays. 1999; 21:486–498. [PubMed: 10402955]

Rudolf A, Buttgereit D, Jacobs M, Wolfstetter G, Kesper D, Pütz M, Berger S, Renkawitz-Pohl R, Holz A, Önel SF. Distinct genetic programs guide Drosophila circular and longitudinal visceral myoblast fusion. BMC Cell Biol. 2014; 15:27. [PubMed: 25000973]

Sato T, van Es JH, Snippert HJ, Stange DE, Vries RG, van den Born M, Barker N, Shroyer NF, van de Wetering M, Clevers H. Paneth cells constitute the niche for Lgr5 stem cells in intestinal crypts. Nature. 2011; 469:415–418. [PubMed: 21113151]

Schröter RH, Buttgereit D, Beck L, Holz A, Renkawitz-Pohl R. Blown fuse regulates stretching and outgrowth but not myoblast fusion of the circular visceral muscles in Drosophila. Differentiation. 2006; 74:608–21. [PubMed: 17177857]

Scopelliti A, Cordero JB, Diao F, Strathdee K, White BH, Sansom OJ, Vidal M. Local control of intestinal stem cell homeostasis by enteroendocrine cells in the adult Drosophila midgut. Curr Biol. 2014; 24:1199–1211. [PubMed: 24814146]

Scoville DH, Sato T, He XC, Li L. Current view: intestinal stem cells and signaling. Gastroenterology. 2008; 134:849–864. [PubMed: 18325394]

Singh SR, Liu W, Hou SX. The adult Drosophila malpighian tubules are maintained by multipotent stem cells. Cell Stem Cell. 2007; 1:191–203. [PubMed: 18371350]

Singh SR, Zeng X, Zheng Z, Hou SX. The adult Drosophila gastric and stomach organs are maintained by a multipotent stem cell pool at the foregut/midgut junction in the cardia (proventriculus). Cell Cycle. 2011; 10:1109–1120. [PubMed: 21403464]

Struhl G, Basler K. Organizing activity of wingless protein in Drosophila. Cell. 1993; 72:527–540. [PubMed: 8440019]

Szotek PP, Chang HL, Zhang L, Preffer F, Dombkowski D, Donahoe PK, Teixeira J. Adult mouse myometrial label-retaining cells divide in response to gonadotropin stimulation. Stem Cells. 2007; 25:1317–1325. [PubMed: 17289934]

Takashima S, Mkrtchyan M, Younossi-Hartenstein A, Merriam JR, Hartenstein V. The behaviour of Drosophila adult hindgut stem cells is controlled by Wnt and Hh signalling. Nature. 2008; 454:651–655. [PubMed: 18633350]

Takashima S, Younossi-Hartenstein A, Ortiz PA, Hartenstein V. A novel tissue in an established model system: the Drosophila pupal midgut. Dev Genes Evol. 2011a; 221:69–81. [PubMed: 21556856]

Takashima S, Adams K, Ortiz PA, Ying C, Moridzadeh R, Younossi-Hartenstein A, Hartenstein V. Development of the Drosophila entero-endocrine lineage and its specification by the Notch signaling pathway. Dev Biol. 2011b; 353:161–172. [PubMed: 21382366]

Takashima S, Paul M, Aghajanian P, Younossi-Hartenstein A, Hartenstein V. Migration of Drosophila intestinal stem cells across organ boundaries. Development. 2013; 140:1903–1911. [PubMed: 23571215]

Takashima S, Paul M, Aghajanian P, Younossi-Hartenstein A, Hartenstein V. Origin and dynamic lineage characteristics of the developing *Drosophila* midgut stem cells. Dev Biol. 2016; doi: 10.1016/j.ydbio.2016.06.018

Tang Z, Wang A, Yuan F, Yan Z, Liu B, Chu JS, Helms JA, Li S. Differentiation of multipotent vascular stem cells contributes to vascular diseases. Nat Commun. 2012; 6(3):875.

Tepass U, Hartenstein V. Epithelium formation in the Drosophila midgut depends on the interaction of endoderm and mesoderm. Development. 1994; 120:579–590. [PubMed: 8162857]

Thomas K, Engler AJ, Meyer GA. Extracellular matrix regulation in the muscle satellite cell niche. Connect Tissue Res. 2015; 56:1–8. [PubMed: 25047058]

Tribioli C, Frasch M, Lufkin T. Bapx1: an evolutionary conserved homologue of the Drosophila bagpipe homeobox gene is expressed in splanchnic mesoderm and the embryonic skeleton. Mech Dev. 1997; 65:145–162. [PubMed: 9256352]

Xu N, Wang SQ, Tan D, Gao Y, Lin G, Xi R. EGFR, Wingless and JAK/STAT signaling cooperatively maintain Drosophila intestinal stem cells. Dev Biol. 2011; 354:31–43. [PubMed: 21440535]

Yen TH, Wright NA. The gastrointestinal tract stem cell niche. Stem Cell Rev. 2006; 2:203–212. [PubMed: 17625256]

Zitserman D, Roegiers F. Live-cell imaging of sensory organ precursor cells in intact Drosophila pupae. J Vis Exp. 2011; 27(51)

Highlights

- Drosophila visceral muscle fibers directly descends from larval fibers
- Larval visceral muscles dedifferentiate into “secondary myoblasts”, losing their myofibrils and extracellular matrix,
- secondary myoblasts re-differentiate into adult syncytia in the late pupa
- intestinal morphogenesis is dependent on the presence of the visceral muscle;
- proliferation of presumptive intestinal stem cells depends on the presence of visceral muscle.

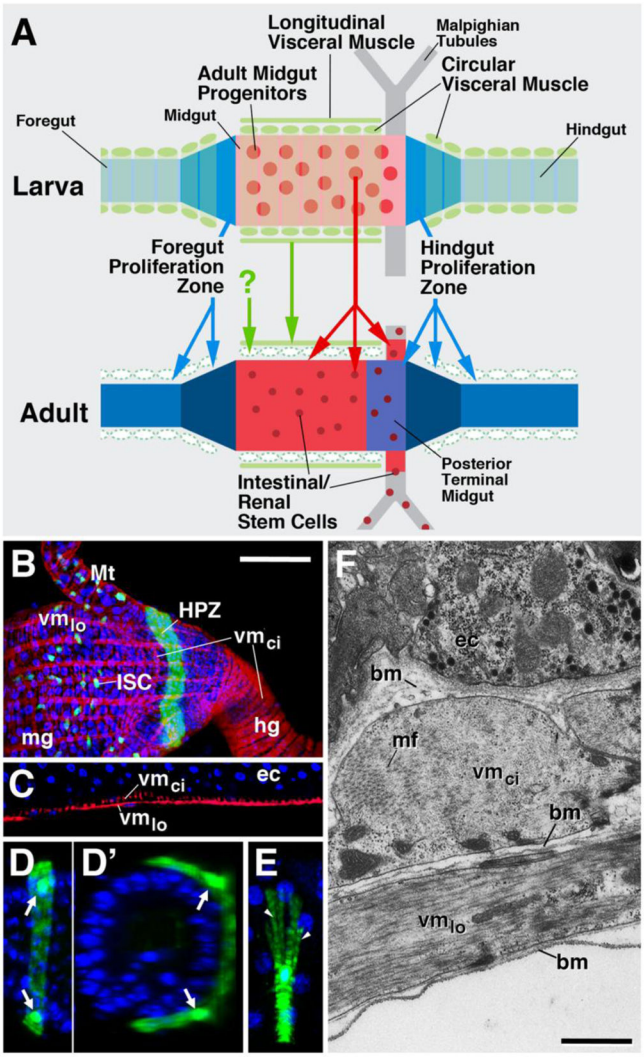

Fig. 1.

Development and architecture of the visceral musculature of the adult *Drosophila* intestine. (A) Schematic representation of the Drosophila intestine, indicating ontogenetic relationship between larval and adult structures. (B) Tangential confocal section of adult midgut/hindgut boundary domain. Myofibrils are marked with phalloidin (red). Blue label (Topro) in this panel and in (C–E) marks cell nuclei. Intestinal stem cells (ISCs) of the adult midgut and the hindgut (concentrated in hindgut proliferation zone, HPZ) are labeled by Stat92E-GFP (green). (C) Longitudinal confocal section of midgut wall, depicting enterocyte layer (ec), circular muscle layer (vm_{ci}) and longitudinal muscle layer (vm_{lo}). (D, D′,E) Single fiber clones of circular muscle (green) of late pupal midgut. (D) Tangential section, showing muscle fiber with two nuclei (arrows). (D′) cross section of the same fiber. (E) Tangential section, high magnification, showing assembly of 4–5 myofibrils (arrowheads) in circular muscle fiber. (F) Electron micrograph of longitudinal section of adult hindgut, showing enterocyte (ec), basement membrane (bm), circular muscle (vm_{ci}) and longitudinal muscle (vm_{lo}). Abbreviations used in this and the following figures: ahg adult hindgut; aHPZ adult

hindgut proliferation zone; amp, adult midgut progenitor; bm, basement membrane; cd cell death; ec enterocyte; ec_{ad} adult enterocyte; ec_{lv} larval enterocyte; hg, hindgut; HPZ, hindgut proliferation zone; HPZ>ahg larval hindgut proliferation zone while extending to become the adult hindgut epithelium; ISC, intestinal stem cell; lhg larval hindgut; mf myofilament; mg, midgut; mgpo posterior domain of the midgut; mp macrophage; Mt, Malpighian tubules; pl plug; pmg transient pupal midgut; pv proventriculus; re rectum; tr trachea; ure ureter; vm_{ci}, circular visceral muscle; vm_{lo}, longitudinal visceral muscle; yb yellow body. Bars: 50μm (A, C–E, G); 10 μm (B); 1 μm (F)

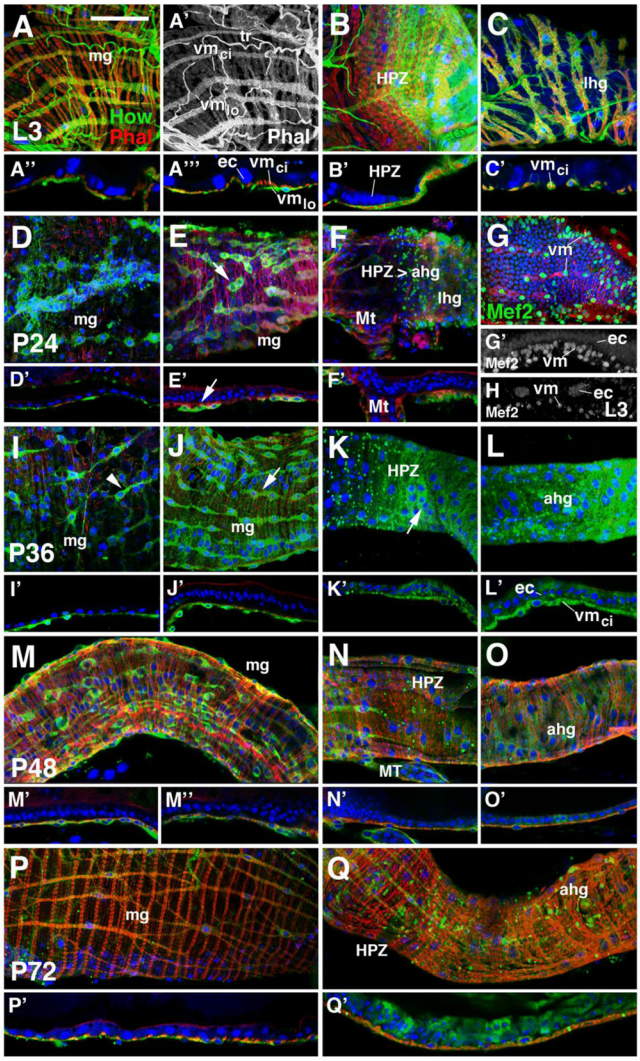

Fig. 2.

Metamorphosis of the visceral musculature. All panels show Z-projections of tangential or longitudinal confocal sections of gut preparations in which phallodin (red) labels myofibrils, and How-Gal4>UAS-mcd8-GFP (green) the cytoplasm of muscle cells. Blue label (Topro) shows cell nuclei. Panels of the left column (A-A‴, D–E′, I–J′, M-M″, P-P′) depict midgut; panels in the middle (B-B′, F-F′, K-K′, N-N′, Q-Q′) show midgut hindgut boundary; panels at the right (C-C′, L-L′, O-O′) hindgut. (A–C′) Late third instar larva (L3). Tangential sections (A–C) and longitudinal sections (A″–C′), showing intact larval circular and longitudinal visceral muscle fibers. Note (panel A′) that How-Gal4 is expressed in both longitudinal visceral fibers (vm_{lo}; high level of expression) and circular fibers (vm_{ci}; low level). (D–F′) 24h after puparium formation (P24). Visceral muscle of midgut (D–E′), and hindgut-midgut boundary region [hindgut proliferation zone (HPZ)] and hindgut (lhg) (F-F′) show decreased labeling and irregular patterning. Many longitudinal muscle fibers have dissociated into short chains of cells [arrow in (E, E′)]. (G–H) Antibody against muscle determinant Mef2 shows strong signal (green) in visceral muscle nuclei of P24 intestine. Expression is upregulated compared to L3 stage (compare G and H). (I–L′) At 36h after

puparium formation (P36) phalloidin-positive myofibrils have disappeared. How-Gal4-positive cells (“secondary myoblasts”) remain intact. Myoblasts of longitudinal visceral muscle fibers form single cells [arrowhead in (I)] or chain of cells [arrow in (J)]. In hindgut, secondary myoblasts of circular fibers form dense layer [arrow in (K)] surrounding metamorphosing midgut epithelium [enterocytes (ec)]. (M–O′) Rebuilding of adult visceral musculature at 48h after puparium formation (P48). Phalloidin-positive myofibrils have reappeared, but are still thin and irregular in trajectory. (P–Q′) At 72h after puparium formation (P72) visceral muscle has acquired its adult pattern that is maintained through the rest of metamorphosis and the adult stage. For other abbreviations, see legend of Figure 1. Bar: 50μm (A–O′)

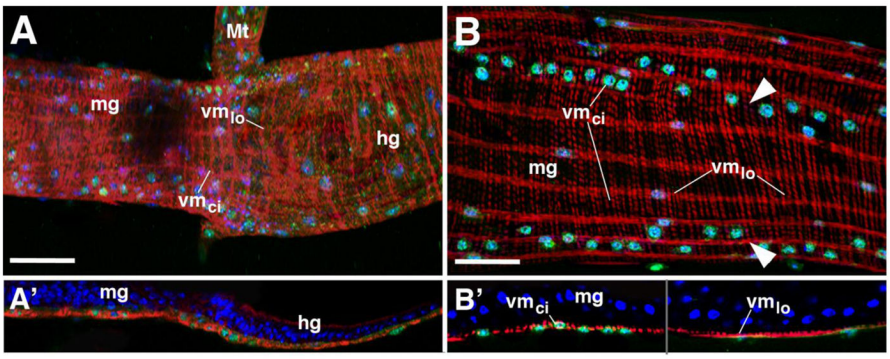

Fig. 3.

The larval visceral muscle persists through metamorphosis. Tangential (A, B) and longitudinal (A –B′) confocal sections of adult midgut-hindgut boundary region. Myofibrils are labeled by phalloidin (red). Cellular nuclei labeled by Topro (blue). Lineage tracing construct (*Act5C>stop>lacZ*; green), activated by How-Gal4 at the larval stage, appears in adult muscle fibers. For abbreviations, see legend of Figure 1. Bars: 50μm (A, A′); 25μm (B. B′)

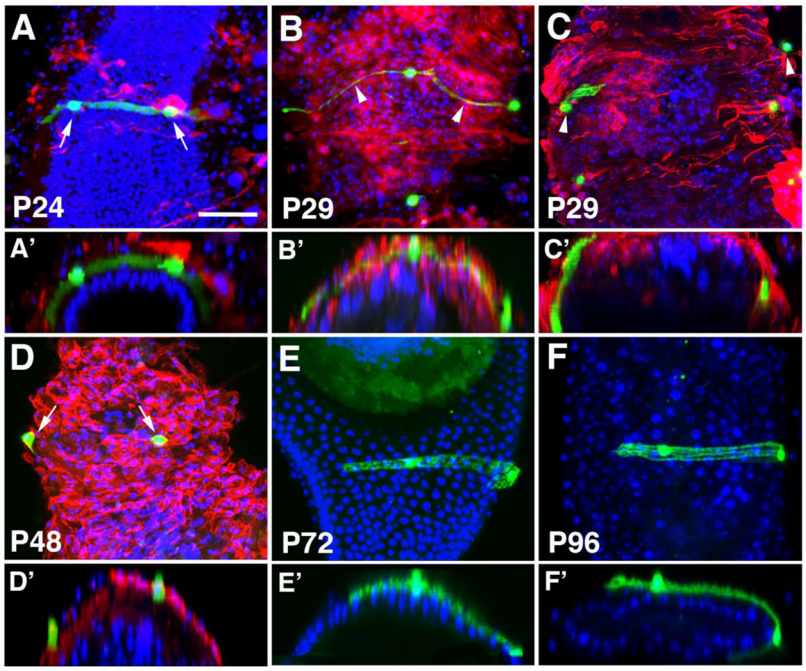

Fig. 4.

Clonal analysis of persisting visceral muscle fibers. Z-projections of confocal sections of pupal midgut containing single fiber circular muscle clones (labeled by GFP; green) during various stages of metamorphosis. (A–C, D–F): Tangential sections; (A –C′; D –F′): cross sections of same preparations shown in (A–F). Myofibrils are labeled by phalloidin (red) in A–D′; cellular nuclei labeled by Topro (blue). (A, A′) At 24h after puparium formation (P24) circular muscle fibers carried over from the larval period are still syncytia with two nuclei (arrows). (B–C′) Clones fixed at 29h after puparium formation (P29). Syncytia are in the process of breaking up (B, B′); arrowheads point at thin cytoplasmic bridges still connecting the two nuclei. In most cases, clones are represented by single cells [secondary myoblasts; arrowheads in C)]. (D, D′). Single cell secondary myoblasts still exist at P48. (E–F′). In the late pupa (E, E: P72; F, F: P96) GFP-label induced in larval visceral muscle again appears in syncytial, binucleate adult visceral muscle fibers. Bar: 50μm (A, E, K, N); 25μm (B–D′, F–J′,L–M′, O–P′).

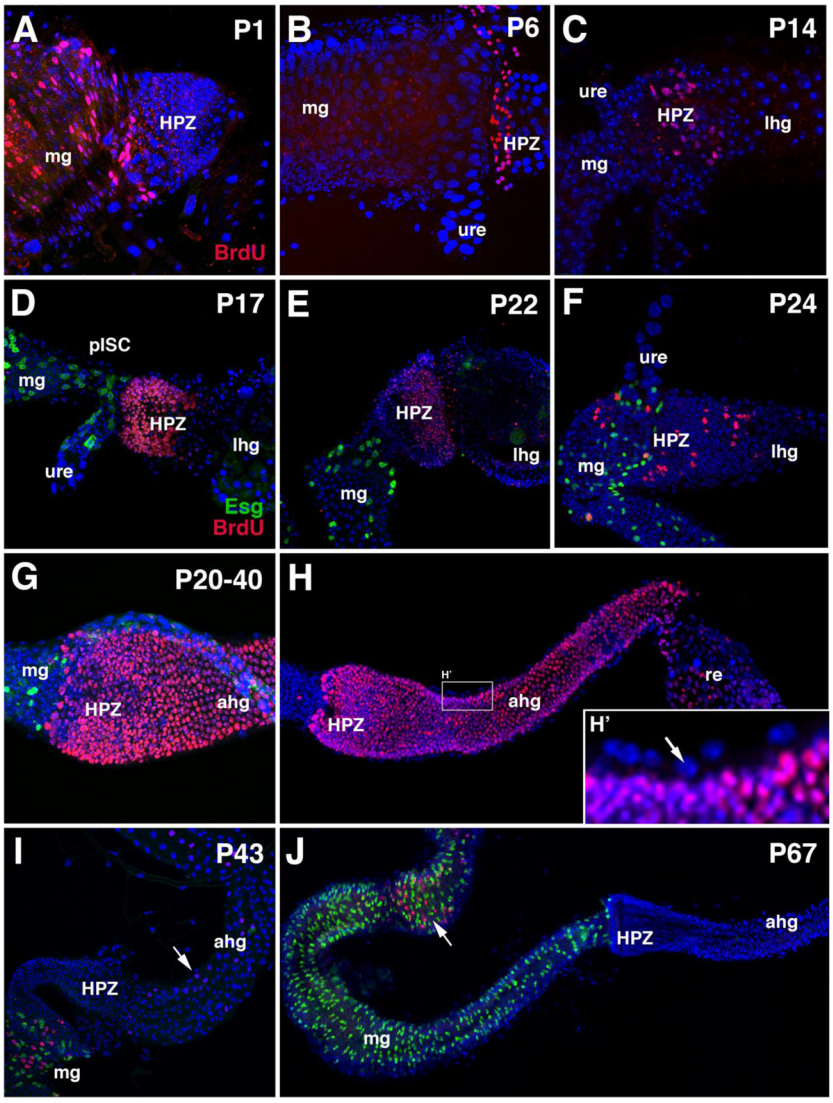

Figure 5.

Proliferation of the HPZ during metamorphosis. Z-projections of confocal sections of midgut-hindgut domain of pupal guts that had been pulsed with a BrdU injection at the time indicated at upper right hand corner of panel. All preparations were fixed and dissected 2–3hrs after injection; except for specimen shown in (G, H), which were fixed after 20hrs. Specimens were labeled with anti-BrdU (red), Topro (nuclei; blue) and Esg-Gal4>UAS-mcd8GFP (midgut intestinal stem cells; green). The hindgut proliferation zone (HPZ) undergoes a round of BrdU incorporation during early metamorphosis (P6–P17), and another round during the time when the HPZ elongates to form the adult hindgut (P24–40; F–H). No BrdU incorporation into hindgut enterocytes occurs after this stage. Proliferation does occur in subsets of midgut ISCs [arrows in (I, J)]. No BrdU incorporation is observed in muscle nuclei at any stage; arrow in H points at Topro-labeled, BrdU-negative muscle nuclei adjacent to BrdU-positive hindgut epithelium. For other abbreviations, see legend to Fig. 1.

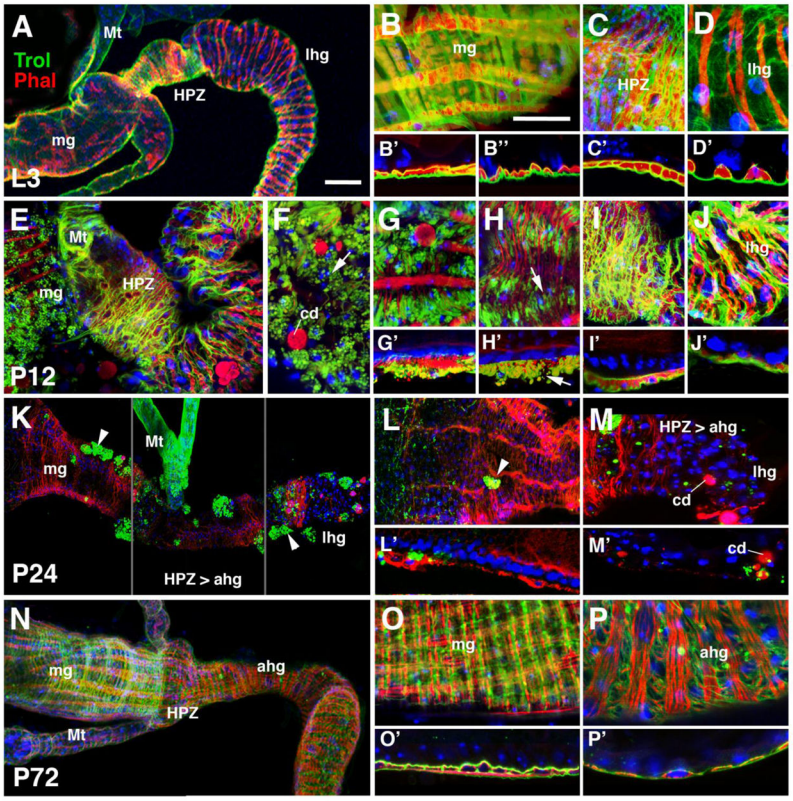

Figure 6.

Metamorphosis of the basement membrane surrounding visceral muscle fibers. Panels show tangential confocal sections (A–P) or longitudinal sections (B – P′) of the midgut-hindgut boundary region at the late larval stage (L3; A–D′), 12h after puparium formation (P12; E–J′), 24h after puparium formation (P24; K–M′) and 72h after puparium formation (P72; N–P′). Myofibrils are labeled by phallodin (red); basement membrane is labeled by reporter Trol-GFP (green). Nuclei are labeled by Topro (blue). (A–D′) Larval circular and longitudinal fibers are surrounded on all sides by basement membrane. (E–J′) At 12h after puparium formation (P12), basement membranes break down; Trol-GFP signal reveals fragments of extracellular material surrounding circular fibers [arrows in (F, H, H′)]. (K–M′) In 24h pupa, basement Trol-GFP signal has disappeared from around visceral fibers. Macrophages (arrowheads) contain Trol-GFP-positive material, indicating that these cells are involved in digesting basement membranes. Note intact covering of ureter and proximal Malpighian tubules [Mt in (K)] by basement membrane. (N–P′). Basement membranes have been re-established in the 72h pupa around adult visceral muscle fibers. Note that the hindgut [ahg in N, P, P′) lags behind the midgut (mg) with regard to regaining a strong Trol-GFP signal, indicating that basement membrane may from later in this region, compared to the midgut. For other abbreviations see legend of Figure 1. Bars: 50μm (panels of left column; A, E, F, F′, K, N); 25μm (panels of middle and right column; B–D′; G–J′; L–M′; O–P′).

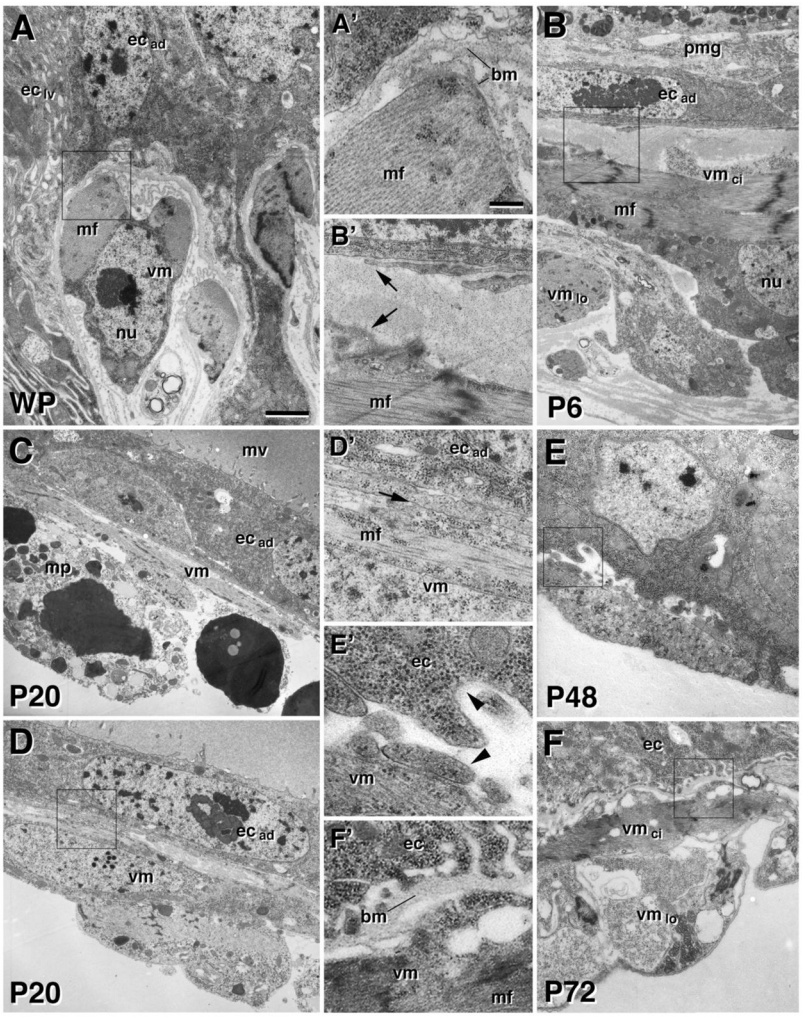

Figure 7.

Ultrastructure of the visceral muscle and basement membrane during metamorphosis. (A–F) Electron micrographs of cross sections of the midgut wall in the white prepupa (WP; A, A′), 6h pupa (P6, B, B′), 20h pupa (P20, C–D′), 48h pupa (P48, E, E′) and 72h pupa (P72, F, F′). Square outlines in panels taken at low magnification (A–F) indicate regions shown at high magnification in panels A –F′). (A, A′) In white prepupa, most adult enterocytes (ec_{ad}) have become epithelial cells and push in between larval enterocytes (ec_{lv}). The midgut wall is thrown into circular folds, housing visceral muscle fibers (vm; nu indicates nucleus of visceral muscle fiber). Note in (A′) massive basement membrane (bm) surrounding muscle fiber. At P6 (B, B′), adult enterocytes form a complete epithelium composed of flat cells, surrounding the transient pupal midgut (pmg). Circular and longitudinal muscle fibers with myofilaments (vm_{ci}, vm_{lo}, respectively) are still intact. However, extracellular material appears as a electron-lucent mass of floccular material [arrows in (B′)]. (C–D′) At P20, visceral muscle fibers are almost devoid of myofilaments. Basement membranes are absent, as indicated by arrow in (D′) which points at the juxtaposed membranes of a visceral muscle cell (vm) and the process of an enterocyte without any intervening extracellular material. (E, E′) At P48, a thin layer of extracellular material is again present around the basal surface of

enterocytes (ec) and visceral muscle (vm). (F′ F′) By P72, a regular basement membrane is present. For other abbreviations, see legend of Figure 1. Bars: 1μm (A–F); 0.25μm (A –F′).

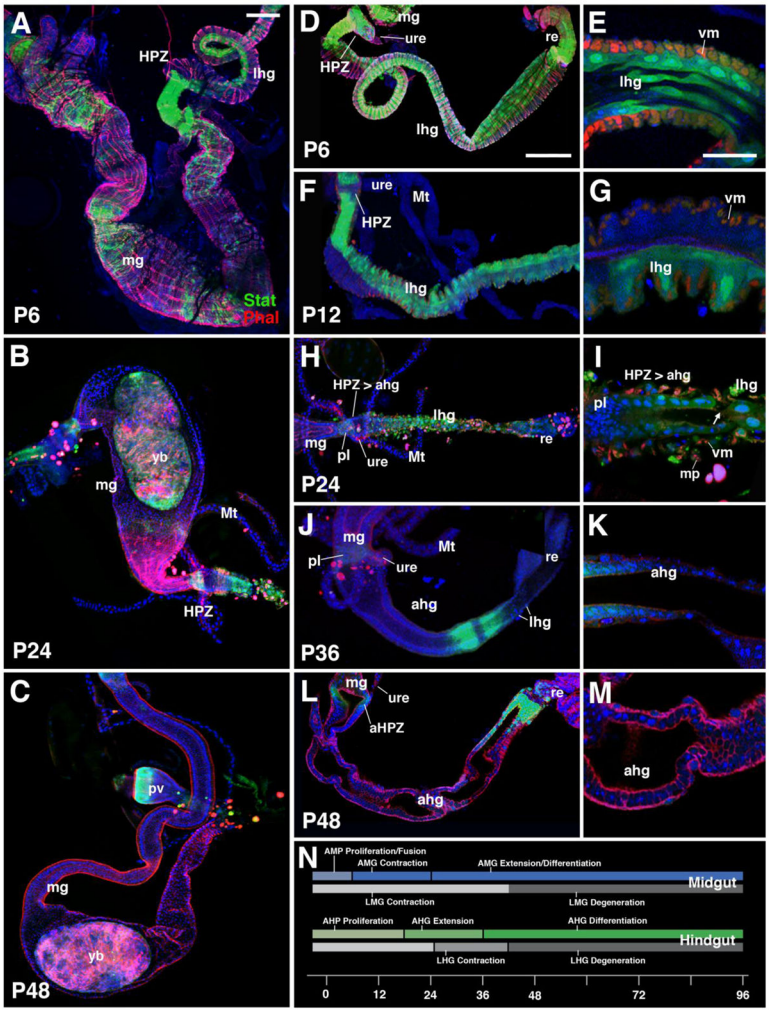

Figure 8.

Morphogenesis of the midgut and hindgut during metamorphosis. Z-projections of longitudinal confocal sections of preparations labeled with phalloidin (visceral muscle fibers; red), Topro (nuclei; blue) and Stat92E-GFP (green). Left column (A–C) presents low magnification images of the midgut. Note dramatic shortening of the midgut during early metamorphosis (B), followed by an elongation around 48h after puparium formation (P48 in C). Stat92E-GFP labels enterocytes of transient pupal midgut which forms a layer around the degenerating larval midgut [yellow body, yb in (B and C)]. Middle column (D, F, H, J, L) shows low magnification views of the hindgut, and right column (E, G, I, K, M) presents high magnification views of the hindgut. At P6 (D) and P12 (F), the hindgut is still formed mostly of larval cells (lhg), the hindgut proliferation zone (HPZ; strongly positive for Stat92E-GFP) is limited to a short domain at the anterior end of the hindgut. At P24 (H, I) massive amounts of macrophages (mp) accumulate around the remainder of the larval hindgut, which retreats posteriorly. Arrow in (I) points at the boundary between larval hindgut enterocytes and adult enterocytes of the advancing HPZ. At P36 (J, K) the hindgut tube consists of almost exclusively adult enterocytes; larval hindgut cells (lhg in J) are restricted to a short domain at the boundary towards the rectum (re). At P48 (L, M) the adult

hindgut has been completed and elongated. Note absence of phalloidin-positive visceral muscle around midgut and hindgut at P24 and P36, and presence of adult muscle layer at P48. (N) Time lines of morphogenetic events shaping the midgut (upper line) and hindgut (lower line); units in hours after puparium formation. For other abbreviations, see legend of Figure 1. Bars: 50μm (A–C); 100μm (D, F, H, J, L); 25μm (E, G, I, K, M).

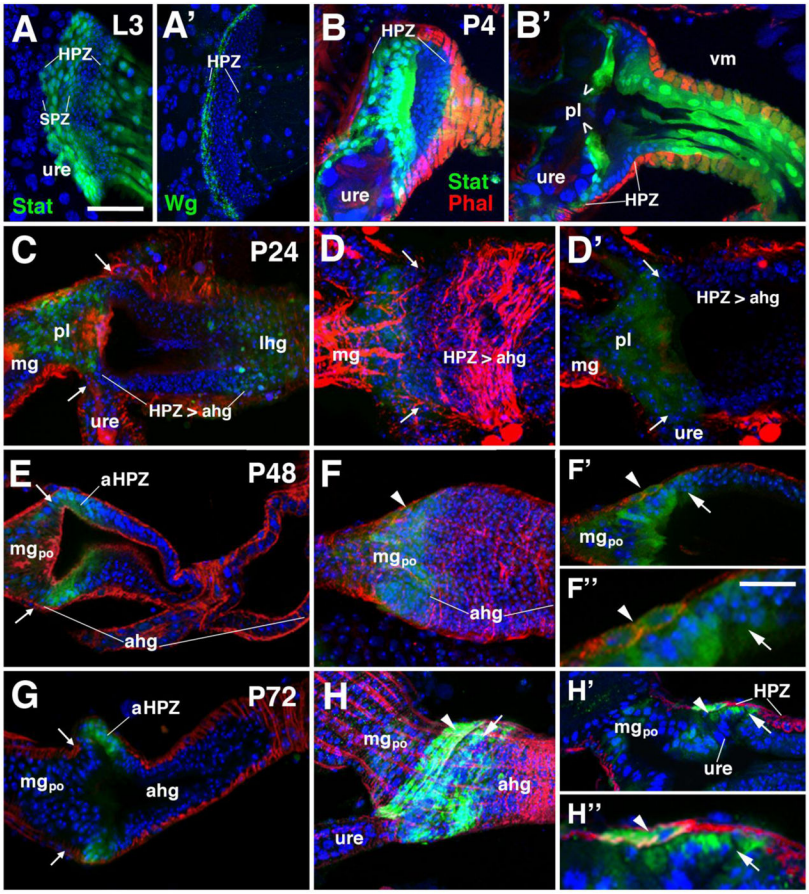

Figure 9.

Renewal of the hindgut proliferation zone during metamorphosis. Z-projections of longitudinal [left column; C, E, G) and right column (B′, D′, F′, F″, H′, H″)] and tangential confocal sections (A, A′, B, D, F, H) of the midgut-hindgut boundary region. Represented are the late larva (L3; A, A′), 4h pupa (P4; B, B′), 24h pupa (P24; C–D′), 48h pupa (P48; E–F″) and 72h pupa (P72; G–H″). Phalloidin (red) labels myofibrils; Topro (blue) cell nuclei. In panels at the top and to the left (A, B, B′, C, E, G), Stat92E-GFP (green) labels hindgut proliferation zone (HPZ); all other panels (A′, D, D′, F, F′, F′, H, H′, H″) show expression of the *wg*-lacZ reporter (green). (A) In the late larva, high level of Stat expression appears in a sharply demarcated stripe in the anterior part of the HPZ, called the spindle cell zone (SCZ). Wg transcript appears in a 1–2 cell wide belt at the anterior border of the HPZ (A′). During early metamorphosis, these cells undergo an epithelial-mesenchymal transition (B′) and become the "plug" [pl in (B′, C); small arrows in D–G demarcate boundary between plug and presumptive adult hindgut], which eventually re-epithelializes as the posteriormost domain of the adult midgut [mg_{po} in (E, G)]. During this phase, Stat expression in the plug/posterior midgut domain declines. A new sharply demarcated band of Stat expression appears at the anterior boundary of the emerging adult hindgut around P48 [aHPZ in (E, G)]. The expression of *wg*-lacZ follows a similar dynamics. As the *wg*-lacZ-positive cells get incorporated into the plug (D, D′) and, subsequently, the adult midgut (F, F′), *wg*-lacZ signal is downregulated. A new, strong *wg*-

lacZ signal reappears around P48, first in a narrow band of visceral muscle (arrowheads in F′, F″, H′, H″), followed by posteriorly adjacent epithelial cells (large arrow in H-H). For other abbreviations, see legend of Fig. 1. Bars: 50μm (A–H); 25μm (F″, H″).

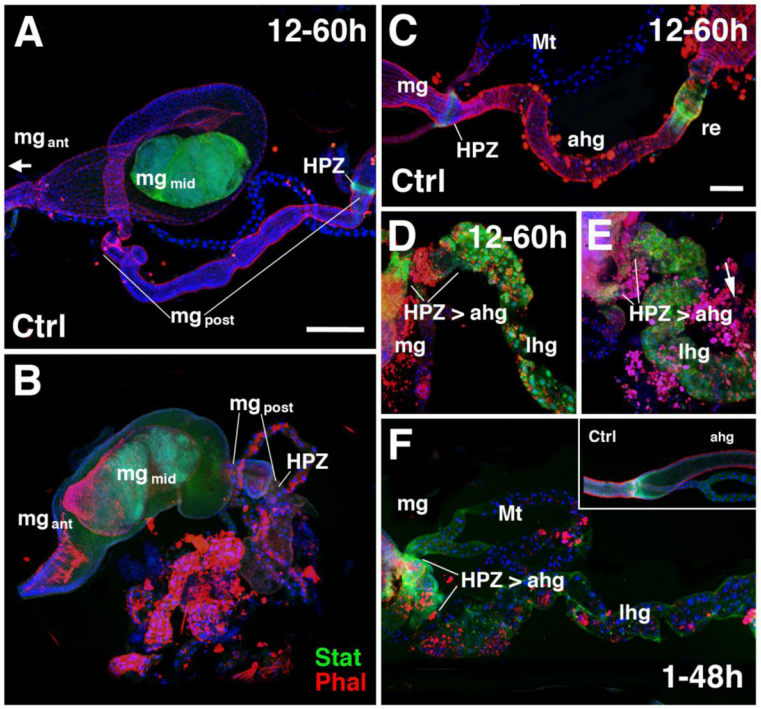

Figure 10.

The effect of muscle ablation on gut morphogenesis. Z-projections of longitudinal confocal sections of late pupal midgut (A, B) or hindgut (C–F) of control (A, C, inset in F) and experimental animals (B, D–F) in which visceral musculature was ablated by expressing UAS-hid; rpr under the control of tub-Gal80^{ts}; How-Gal4. All animals were kept at 18°C until pupariation (F) or 12h after puparium formation (A–E), after which temperature was raised to 29°C to activate the UAS-hid;rpr construct. Preparations are labeled with phalloidin (red; myofibrils), Topro (nuclei; blue) and Stat92E-GFP (green). Note reduced length of experimental midgut (B). In hindgut of experimental animals, larval hindgut cells (lhg), recognizable by their large size, remain, and HPZ does not expand. For other abbreviations, see legend of Fig. 1. Bars: 100μm (A, B); 50μm (C–F).

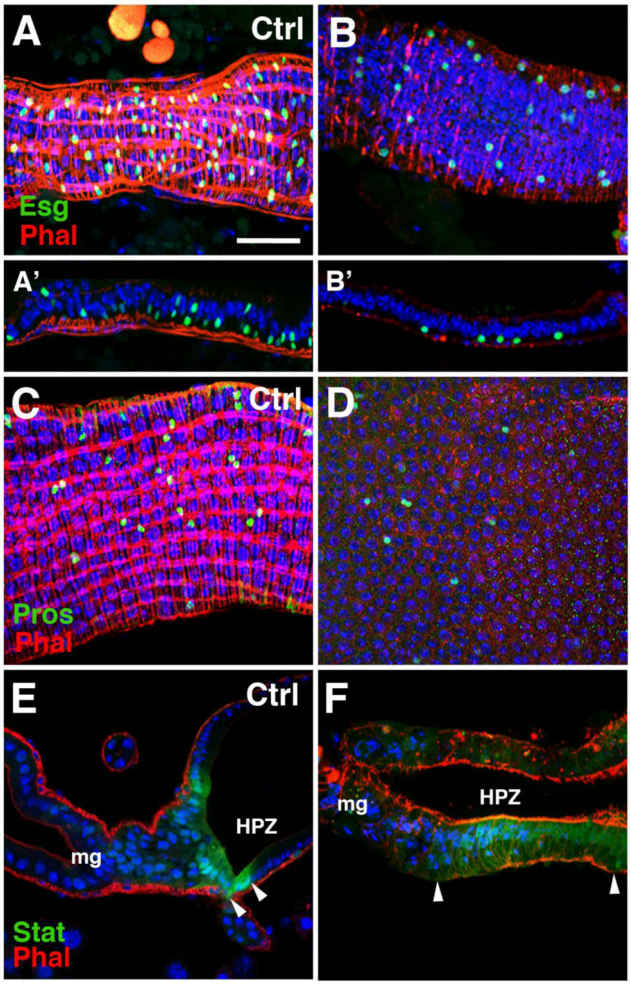

Figure 11.

The effect of muscle ablation on the formation of intestinal stem cells. Z-projections of tangential (AD) and longitudinal (A′, B′; E, F) confocal section of late pupal midgut (A–D) and midgut-hindgut domain (E, F); left column (A/A′, C, E) shows control; right column (B/B′, D, F) shows preparations after ablating visceral muscle by UAS-hid;rpr active during a time interval of 12–60h after puparium formation. Labeling includes phalloidin (myofibrils; red), Topro (nuclei; blue), Esg-Gal4>UAS-mcd8-GFP [midgut intestinal stem cells (ISCs); green (in A, B)], anti-Prospero [Pros; endocrine cells; green in (C, D)], and Stat92E-GFP [HPZ; green in (E, F)]. Note significant reduction in number of ISCs and endocrine cells in experimental animals. Expression of Stat, confined to a narrow band [arrowheads in (E)] demarcating the adult spindle cell zone, is spread out over a wide domain in experimental animal [arrowheads in F)]. Note that faint phalloidin signal in experimental guts corresponds to (mostly apical) cortical microfilament bundles within enterocytes, rather than muscle fibers surrounding the epithelium basally. For other abbreviations, see legend of Fig. 1. Bar: 50μm (A–F).